RSC Advances

ROYAL SOCIETY OF CHEMISTRY

www.rsc.org/advances

Enhanced visible-light-driven photoactivities of single-walled carbon nanotubes coated with N doped TiO_2 nanoparticles

Tianyu Gao[1], Guocheng Sun[1], Feiyue Cheng[1], Ke Dai[1*], Hao Chen[2*], Kejian Deng[3], Qiaoyun Huang[1]

[1] College of Resources and Environment, Huazhong Agricultural University, Wuhan 430070, P R China

[2] College of Science, Huazhong Agricultural University, Wuhan 430070, P R China

[3] Key Laboratory of Catalysis and Materials Science of the State South-Central University for Nationalities, Wuhan 430074, P R China

Abstract: A two-step hydrothermal method is used to prepare N doped single-walled carbon nanotube-TiO_2 (SWCNT-N/TiO_2) hybrids with different contents of SWCNTs from 1.25 wt% to 10 wt%. The photocatalysts were characterized by X-ray diffraction analysis, UV-vis diffuse reflectance spectroscopy, Raman spectroscopy, scanning electron microscopy, transmission electron microscopy, and X-ray photoelectron spectroscopy. The UV-vis diffuse reflectance spectra show an apparent enhancement of absorption throughout the visible light region. Raman spectroscopy further confirms the chemical interaction between the N/TiO_2 and SWCNTs in the hybrid. SWCNT-N/TiO_2 hybrid presents a superior photocatalytic activity to DWCNT-N/TiO_2 (N doped double-walled carbon nanotube-TiO_2) and MWCNT-N/TiO_2 (N doped multi-walled carbon nanotube-TiO_2) based on the results of the photocatalytic degradation of sulfathiazole under visible light irradiation, which is attributed to the synergetic effects of SWCNT modification and N doping. N doping

* Corresponding author. Tel: +86-27-8767-1033; Fax: +86-27-8728-2137.
E-mail address: dk@mail.hzau.edu.cn (K. Dai). hchenhao@mail.hzau.edu.cn (H. Chen).

induces visible light absorption by either introducing localized electronic states within the band gap or contributing electrons to the valence band and metal-like SWCNT can act as an electron conductor to facilitate the fast injection of the photogenerated electrons on the conduction band of N/TiO_2, leading to significantly enhanced visible-light-driven photocatalytic activity.

1. Introduction

Photocatalysis is a potential technology in meeting cleaning energy demand and environmental remediation [1-2]. Recently, many researchers applied the photocatalysis to remove organic pollutants in aqueous suspension and demonstrated that the photocatalyst displayed a good removal effect on those pollutants [3-5]. By far, TiO_2 has emerged as the most promising photocatalyst because of its high oxidative power, photostability, low cost, and nontoxicity. However, the band gap energy (E_g=3.2 eV) of the anatase TiO_2 is a major disadvantage for its application, since the photocatalytic process can only be initiated under UV irradiation (which is only approximately 4% of solar radiation). Moreover, the low quantum efficiency caused by fast recombination of photogenerated h^+-e^- pairs is another drawback when TiO_2 is used to be a photocatalyst. In overcoming the above disadvantages, modification on TiO_2 has drawn a lot of attention from researchers. Doping with metal/nonmetal elements and surface modification with semiconductor of narrow band-gap are both typical approaches to generate visible-light-driven photoactivity from TiO_2. Among the nonmetal dopants, nitrogen has been considered as an effective dopant since N doped TiO_2 (N/TiO_2) was synthesized firstly by Asahi et al. [6]. N/TiO_2 has a new energy band gap lower than pristine TiO_2 owing to the mixing of the 2p nitrogen level with the oxygen 2p orbital to form the valence band.

Consequently, the rate of recombination of h^+-e^- pairs is higher, which remains a serious obstacle to achieving high visible-light-induced photocatalytic activity. Several studies have investigated techniques to reduce the electron-hole combination rate via metal coating/doping [7, 8]. Noble metal nanoparticles can effectively enhance the charge carrier separation by forming a Schottky barrier on the surface of TiO_2. In addition, generation of surface plasmon resonance can help to shift the absorption of the TiO_2 in the visible region [8].

In the recent years, carbon nanotubes (CNTs) has received growingly considerable attention on the field of photocatalysis due to its unique electronic and physical properties [9, 10], which could act as an electron acceptor because of the conductive structure of CNTs scaffolds and hence induced efficient charge transfer [11, 12]. It is expected that CNTs may also act as effective electron sinks because of its high electrical conductivity and electron storage capacity which was demonstrated by Yu et al. [13, 14]. Wang et al. [15] argued that CNTs was utilized to be a photosensitizer which can enhance the visible-light-driven photocatalytic activity of TiO_2. However, we reported the functionalized single-walled carbon nanotubes (SWCNTs) coated with TiO_2 nanoparticles via hydrothermally method where SWCNTs act as an electrical conductor rather than photosensitizer, achieving the improved photoactivity [16]. Although, Studies always focused more on the multi-walled carbon nanotube-TiO_2 (MWCNT-TiO_2) than SWCNT-TiO_2 [13, 17-18], SWCNTs possess a high specific surface area and provides better catalyst-support (dispersal and connection) than MWCNTs, which can achieve a better understanding of the proposed mechanisms [19]. As a novel material, SWCNT-TiO_2 has been fabricated by various ways [20]. Zhou et al. [21] prepared SWCNT-TiO_2 by a facile sol–solvothermal method suggesting that TiO_2 and SWNCTs linked compactly

through ester bonds and thus improved their interfaces which could diminish rate of h^+-e^- pair's recombination. Vajda et al. [22] synthesized SWCNT-TiO_2 by the aid of ultrasonication method and got the optimal composition of the SWCNT-TiO_2 for the degradation of phenol under UV irradiation. However, the enhancement on the photoactivity of TiO_2 after the introduction of SWCNTs is limited under visible light irradiation and the modification of SWCNT-TiO_2 using nitrogen anion to promote photocatalytic activity in the visible light region is less reported.

In this study, we synthesized for the first time a series of SWCNT-N/TiO_2 hybrid by directly growing TiO_2 on the surface of SWCNTs with hydrothermal treatment and then substantial calcination using an N source. The effects of the type of the CNTs (SWCNTs, MWCNTs, and double-walled carbon nanotubes (DWCNTs)) and the contact between CNTs and N/TiO_2 on the visible-light-responsive photoactivity of the CNT-N/TiO_2 hybrids were extensively investigated according to the experimental results of photocatalytic degradation of sulfathiazole under visible light irradiation.

2 Experimental

2.1 Materials

SWCNTs were purchased from Chengdu Organic Chemicals (CAS, China). All other reagents, including Titanium sulfate ($Ti(SO_4)_2$), cetyltrimethylammonium bromide (CTAB), sodium chloride, ethanol, nitric acid and urea were commercially available in analytical purity and used as received.

2.2 Methods

2.2.1 Preparation of SWCNT-N/TiO_2 hybrid

SWCNTs should be pretreated prior to synthesizing the SWCNT-TiO_2 to introduce carboxyl and hydroxyl groups. The detail is shown below: SWCNTs were suspended

in 40 mL deionized water and concentrated nitric acid (volume ratio 7:1), heat stirred for 2 h, followed by rinsing with deionized water until pH value of supernatant became neutral. Next, the dissolved $Ti(SO_4)_2$ was added to the functionalized SWCNTs, CTAB and deionized water (m($Ti(SO_4)_2$): m(CTAB): m(water)=1: 0.12: 100). After stirring for 30 min, the resulting mixture was decanted into a 50 mL stainless steel autoclave for 72 h of hydrothermal treatment at 100 °C. When the suspension cooled down to room temperature, it was centrifuged and rinsed with deionized water and ethanol for 2–3 times. In order to remove the CTAB, ion-exchange treatment was performed by mixing the obtained material with a water and ethanol (molar ratio 1:1) solution of sodium chloride under stirring at ambient temperature for 24 h, then dried at 80 °C overnight. At last, the obtained powder was calcined at 400 °C for 2 h in Muffle Furnace.

The preparation process for the 2.5 wt% SWCNT-N/TiO_2 goes as follows: 0.5 g of SWCNT-TiO_2 and 3.5 g of urea were dispersed in 3 mL deionized water and 1 mL ethanol. The mixture was stirred for 1 h, dried at 80 °C to jelly, and finally calcined at 450 °C for 2 h to obtain SWCNT-N/TiO_2 hybrid. The contents of SWCNTs in the hybrid were controlled at 1.25, 2.5, 5.0, and 10.0 wt%.

2.2.2 Characterization of SWCNT-N/TiO_2 hybrid

X-ray diffraction (XRD) patterns were recorded on the X-ray diffractometer (Bruker Inc., Germany) using Cu Ka radiation source at 35 kV. The UV-vis diffuse reflectance spectroscopy (DRS) of powder solids were collected by a UV-vis spectrophotometer UV-3100 (Shimadzu, Japan) equipped with an integrating sphere using $BaSO_4$ as the reference sample. Raman spectroscopy was performed by using a Confocal Raman Microspectroscopy (Renishaw inc., UK). Transmission electron microscope (TEM) images were obtained on a JEM-2010FEF electron microscope

(JEOL, Japan). Detailed surface images were obtained by means of field emission scanning electron microscope (FESEM) observation on a JEOL-6700F electron microscope. X–ray photoemission spectroscopy (XPS) was carried out by a XSAM800 spectrometer (Kratos Analytical, UK).

2.2.3 Photocatalytic activity of the SWCNT-N/TiO_2 hybrid

The experiment on the photocatalytic degradation of sulfathiazole over SWCNT-N/TiO_2 hybrids in aqueous solution was carried out in a photocatalytic degradation system where a glass reactor was surrounded by circulating water. A 300 W Xenon lamp (PLS–SXE300C, Beijing) with a 420 nm cutoff filter was used as the visible light source, with an average light intensity of 600 μW cm^{-2}. In each experiment, SWCNT-N/TiO_2 hybrid was dispersed in 50 mL of 10 mg mL^{-1} sulfathiazole aqueous solution with a load of 1 g L^{-1}. The suspension was equilibrated for 30 min on a rotating mixer without light, and then exposed to visible light irradiation. At given irradiation time intervals, the mixture was centrifuged at 4000 rpm for 3 min. The supernatant was analyzed with UV-vis spectrophotometer (UV-3100, Shimazu, Japan) by recording the absorbance characteristic band at 282 nm.

3 Results and discussion

3.1 Structure and morphology of the SWCNT-N/TiO_2 hybrid

The effects of N doping and SWCNTs modification on TiO_2 crystallization was investigated by XRD (shown in Figure 1). The diffraction peaks at 2θ values of 25.33°, 37.91°, 48.03°, 54.47°, 55.0°, 62.97° can be indexed to the (101), (004), (200), (105), (211) and (204) planes of anatase phase, respectively [23]. This phenomenon may indicate that dopant did not alter the crystallite structure of TiO_2 but nitrogen

anions have moved into either the interstitial positions (Ti-O-N) or the substitutional sites (O-Ti-N) of the TiO_2 crystal structure [24, 25]. In addition, the characteristic peaks of SWCNTs at 26.6° and 43.5° are not detected in the 1.25 wt% to 10 wt% SWCNT-N/TiO_2 hybrids, which can be attributed to the good dispersion of SWCNTs in the hybrid after surface functionalization [16]. The primary crystallite size of N/TiO_2 and 1.25 wt% to 10 wt% SWCNT-N/TiO_2 hybrids (presented in Table 1) was calculated by the Scherrer equation:

$$d = (0.89 \times \lambda) / \beta \times \cos\theta$$

where d is crystal size, λ is the X-ray wavelength (0.1548 nm for Cu K_α radiation), β is the full width at half-maximum, θ is the diffraction angle associated with the (101) peak. The small grain of TiO_2 nanoparticles in the SWCNT-N/TiO_2 may be attributed to N doping and the introduction of SWCNTs. First, incorporation of nitrogen in TiO_2 crystal lattice result in a decrease in the interplanar distance due to a larger ionic radius (1.46 Å) of N^{3-} ion than O^{2-} ion (1.40 Å) [25]. Moreover, the slow rate of grain growth for TiO_2 in the SWCNT-N/TiO_2 hybrid may be attributed to the introduction of SWCNTs into N/TiO_2, which retards direct contact of the grains. Nevertheless, the particle sizes initially increase and then decrease with increasing concentration of SWCNTs. These experimental results are ascribed to the quantity of contacts N/TiO_2 and SWCNTs, which is influenced by the concentration and the self-aggregation of SWCNTs [16].

The DRS spectra of TiO_2, N/TiO_2, SWCNT-TiO_2, and SWCNT-N/TiO_2 with different contents of SWCNTs are shown in Figure 2a. The spectrum for TiO_2 has an absorption edge at 400 nm, corresponding to a band-gap energy of about 3.1 eV. Compared with pure TiO_2, N/TiO_2, SWCNT-TiO_2 and SWCNT-N/TiO_2 hybrids contain less TiO_2, which leads to a weaker absorption in the UV region. Although the

absorption thresholds of SWCNT-N/TiO_2 hybrids are near to that of TiO_2, all SWCNT-N/TiO_2 hybrids have better absorption in the visible light region (> 400 nm). Compared with the 5 wt% SWCNT-TiO_2, a greater adsorption property of 5 wt% SWCNT-N/TiO_2 hybrid is obtained from the DRS spectra. This phenomenon may demonstrate that nitrogen anions substituted for oxygen positions in the TiO_2 lattice, thereby forming a mid-gap level between the valence and conduction bands of TiO_2 [25].

The band gap energy of TiO_2, N/TiO_2, SWCNT-TiO_2, SWCNT-N/TiO_2 hybrids were calculated by plotting $(ahv)^{0.5}$ versus hv where a is the absorption coefficient (Figure 2b). The results suggest that both SWCNT modification and N doping could narrow the band gap of TiO_2, which lead to a broader optical absorption range; however, the band gap initially narrow and then enlarge with the increase of loading amount of SWCNTs (shown in Table 1), this conclusion indicates that whether the decrease in band gap enhances photocatalytic activity or not depends on the wavelength of incident light [26].

Figure 3 shows the SEM and TEM images of 2.5 wt% SWCNT-TiO_2 and 2.5 wt% SWCNT-N/TiO_2. As shown in Figure 3a and b, the acid-treated SWCNT morphology remain the original structure and is densely covered with a large amount of TiO_2 or N/TiO_2 regardless of nitrogen doping or not, suggesting that TiO_2 or N/TiO_2 was coated on the outer surface of the SWCNTs according to the field emission theory [27]. On the other hand, the N/TiO_2 nanoparticles are homogenously distributed on the surface of acid-treated SWCNTs (Figure 3c) owing to the effect of surface functional groups like carboxyl and hydroxyl, which can contribute to a high specific surface area [28]. Meanwhile, lattice fringes can be clearly seen in TEM image (Figure 3d) indicating that the d spacing for TiO_2 (101) planes is 0.35 nm consistent

with XRD results. Close interfacial contact between N/TiO_2 and the SWCNTs is observed, which is advantageous for transferring electrons and retarding the recombination of photogenerated h^+-e^- pairs, thus improving the photocatalytic activity [21].

Raman spectrum of TiO_2, SWCNTs, 2.5 wt% SWCNT-TiO_2, and 2.5 wt% SWCNT-N/TiO_2 are presented in Figure 4. The characteristic bands at 402.1, 517.4, 636.2 cm^{-1} in the 2.5 wt% SWCNT-N/TiO_2 hybrid corresponding to B_{1g}, A_{1g}, E_g modes of anatase, respectively; no Raman peak due to TiN can be observed in the 2.5 wt% SWCNT-N/TiO_2 hybrid which is in agreement with XRD pattern. Furthermore, our results show an obvious red-shift for the E_g mode of the 2.5 wt% SWCNT-N/TiO_2 hybrid and 5 wt% SWCNT-TiO_2, indicating a decrease naoparticle size according to the report of Zhang et al. [29]. However, compared with 5 wt% SWCNT-TiO_2, the Raman peaks of 2.5 wt% SWCNT-N/TiO_2 hybrid shift to lower frequency due to lattice expansion, which confirm the presence of the dopant anion in the crystal lattice [25]. The characteristic D-band (disordered mode) at 1353 cm^{-1} and G-band (tangential mode) at 1580cm^{-1} of SWCNTs could be observed, indicating the existence of SWCNTs in the hybrid. The relative intensity ratio of the D-band to the G-band is known as an index of graphitization to determine the CNTs microstructure [30]. The I_D/I_G ratio of the hybrid is 0.11 similar to the pure SWCNTs [16], which demonstrates N doping and hydrothermal treatment did not damage the graphitization structure of the 2.5 wt% SWCNT-N/TiO_2 hybrid.

XPS measurements were carried out to further determine the interaction of SWCNTs and N/TiO_2 nanoparticles. Figure 5a presents C 1s, O 1s, Ti 2p, Ti 3s, Ti 3p and N 1s XPS spectrum of 5 wt % SWCNT-N/TiO_2 hybrid. It is observed that C 1s spectrum (Figure 5b) can be fitted to the three peaks, located at 284.6, 285.7, 288.6 eV,

which are ascribed to C-C, C-O, and C-O-O bonds, respectively. The existence of these polar groups demonstrates that the surface of SWCNTs was oxidized to some extent, which is beneficial for the adsorption of the precursor molecules and the nucleation of N/TiO_2 on the surface of SWCNTs [31]. Figure 5c displays the XPS spectrum of Ti 2p for the 5 wt % SWCNT-N/TiO_2 hybrid, which indicates the two peaks at 458.9 and 464.8 eV corresponding to the photo-splitting electrons Ti $2p_{3/2}$ and Ti $2p_{1/2}$, respectively. The binding energies of two peaks presented a blue-shift compared to the CNT/TiO_2 [32], which is attributed to the substitution of a less electronegative nitrogen atom in the place of oxygen in spite of the strong interaction existed between N/TiO_2 nanoparticles and SWCNTs [31]. Furthermore, the O 1s peak for the hybrid appears at 530.0 eV (Figure 5d), suggesting the presence of the substitutional N (O-Ti-N) rather than interstitial N (Ti-O-N) [25]. The N1s spectrum of the hybrid has a main peak at 399.0 eV (Figure 5e), which is greater than the typical binding energy of 396.9 eV in TiN [33], which can be attributed to the 1s electron binding energy of the N atom in the environment of O-Ti-N. This shift to a higher energy is ascribed to the formation of O-Ti-N structure when nitrogen substitutes for oxygen in TiO_2, and hence the electron density around nitrogen is less than in TiN [25].

3.2 Photocatalytic activity

To investigate the contact between the SWCNTs and N/TiO_2 on the visible-light-induced photoactivity of the SWCNT-N/TiO_2 hybrid, homemade TiO_2, N/TiO_2, 5 wt% SWCNT+N/TiO_2 (a simple mixture of SWCNTs and N/TiO_2 at a weight ratio of 1:19) and a series of SWCNT-N/TiO_2 hybrids synthesized by the hydrothermal method were examined in a solution of sulfathiazole under visible light irradiation. The results of degradation efficiency are illustrated in Figure 6. It is

obvious that sulfathiazole was barely decomposed in the absence of photocatalyst. This phenomenon indicates that sulfathiazole elimination by the hydrolysis and/or photolysis can be neglected under visible light irradiation. Photocatalytic degradation of sulfathiazole over homemade TiO_2 was limited because of the low photoactivity of TiO_2 under visible light [34]. Simultaneously, the enhancement on the photoactivity of TiO_2 after the introduction of SWCNTs was inconspicuous. According to Zhou et al. [28], a metal possesses a higher work function than that of the n-type semiconductor (such as TiO_2), electrons can flow from the semiconductor into the metal for adjusting the Fermi energy levels. In general, as-synthesized SWCNTs are composed of one-third metal and two-thirds semiconductor ones; therefore SWCNTs cannot act as photosensitizer to improve the visible-light-induced photoactivity [35]. Nevertheless, N/TiO_2 exhibits a high photoactivity, since substitutional nitrogen forms new state that lies just above the valence band of TiO_2 which causes band gap narrowing enabling it to absorb visible light. [36]. Moreover, the 5 wt% SWCNT+N/TiO_2 showed a slower removal rate of sulfathiazole than the 5 wt% SWCNT-N/TiO_2 hybrid. According to these experimental results, a possible explanation for the higher photoactivity of 5 wt% SWCNT-N/TiO_2 hybrid is the intimate interaction of N/TiO_2 with the SWCNTs and the formation of localized electronic states in the band gap caused by N doping [37]. In our study, the 5 wt% SWCNT-N/TiO_2 hybrid presented superior photoactivity to 5 wt% DWCNT-N/TiO_2 hybrid and 5 wt% MWCNT-N/TiO_2 hybrid (Figure 6). The phenomenon is different from the previous study, according to the report of Liu et al [9], SWCNT-TiO_2 presented less photoactivity than DWCNT-TiO_2 and MWCNT-TiO_2. As we know, the structure of CNTs plays an important role in the photocatalytic process. SWCNTs' architecture provides a network to disperse N/TiO_2 nanoparticles. An increase of photoconversion efficiency

represents the beneficial role of the SWCNTs as conducting scaffold to facilitate the fast injection of the photogenerated electrons on the CB of N/TiO_2 [38]. Furthermore, the photocatalytic activity of the hybrids with varying SWCNTs content was also investigated. As shown in Figure 7, 5 wt% SWCNT-N/TiO_2 demonstrated the highest photoactivity with a degradation rate of approximately 100% after reaction of 1 h. By contrast, the effect of 10 wt% SWCNT-N/TiO_2 was not favorable since the excessive SWCNTs can act as recombination center for h^+-e^- pairs, resulting in depressed photoactivity [16].

Based on the experimental findings and the discussion above, the proposed mechanism for the enhanced photoactivity of SWCNT-N/TiO_2 hybrid is summarized (Figure 8). N/TiO_2 exhibits a relatively lower energy band gap than that of pure TiO_2 for electrons to emit from the up-shifting Fermi level into the SWCNT, which results in the metal-like SWCNT possessing an excess negative charge and the VB of semiconductor (N/TiO_2) an excess positive charge [27]. Therefore, SWCNT-N/TiO_2 hybrid can form a semiconductor–metal junction called a Schottky barrier which offers an effective route of decreasing recombination of photogenerated h^+-e^- pairs [29]. The electrons on SWCNTs can further generate superoxide radical from oxygen. Simultaneously, the produced holes can be transferred from the valence band to the surface of N/TiO_2 where they can directly oxidize organic pollutants or indirectly oxidize them through the formation of hydroxyl radicals [15, 39].

4. Conclusions

N doped and single-walled carbon nanotube modified TiO_2 (SWCNT-N/TiO_2) hybrid was synthesized via a two-step hydrothermal method and analyzed using XRD, DRS, SEM, TEM, Raman, and XPS techniques. SWCNTs in the hybrid were coated

with N/TiO_2 nanoparticles, which decrease the crystallization degree of the anatase and generate an intimate contact between the SWCNTs and N/TiO_2. Compared with N/TiO_2 and SWCNT-TiO_2, the high visible-light-induced photoactivity can be rationalized by the synergetic effects originated from both SWCNT modification and N doping. Moreover, SWCNT-N/TiO_2 hybrid showed better photocatalytic activity than DWCNT-N/TiO_2 and MWCNT-N/TiO_2 in the photocatalytic degradation of sulfathiazole under visible light irradiation. The experimental results demonstrate that the SWCNTs act more as an electrical conductor than a photosensitizer, which efficiently suppress charge recombination, resulting in improving interfacial charge transfer, and eventually enhance the photoactivity of SWCNT-N/TiO_2 hybrid.

Acknowledgements

The research was financially supported by the National Natural Science Foundation of China (21307035), Open Foundation of Key Laboratory of Catalysis and Materials Science of the State Ethnic Affairs Commission and ministry of education, south-central university for nationalities (CHCL12004), and the National Training Programs of Innovation and Entrepreneurship for Undergraduates (201210504130).

Reference:

1 F. Wang, W.G. Wang, X.J. Wang, H.Y. Wang, C.H. Tung, L.Z. Wu, *Angew. Chem. Int. Ed.*, 2011, **50**, 3193-3197.

2 M. Elvington, J. Brown, S.M. Arachchige, K.J. Brewer, *J. Am. Chem. Soc.*, 2007, **129**, 10644-1645.

3 M.N. Abellan, B. Bayarri, J. Gimenez, *J. Costa, Appl. Catal. B.*, 2007, **74**, 233-241.

4 M.N. Abellan, J. Gimenez, S. Esplugas, *Catal. Today*, 2009, **144**, 131-136.

5 W. Baran, J. Sochacka, W. Wardas, *Chemosphere*, 2006, **65**, 1295-1299.

6 R. Asahi, T. Morikawa, T. Ohwaki, K. Aoki, Y. Taga, *Sci.*, 2001, **293**, 269-271.

7 S.S. Zhang, F. Peng, H.J. Wang, H.Yu, S.Q. Zhang, J.A. Yang, H.J. Zhao, *Catal. Commun.*, 2011, **12**, 689-693.

8 R.S. Dhabbe, A.N. Kadam, M.B. Suwarnkar, M.R. Kokate, K.M. Garadkar, *J. Mater Sci: Mater. Electron.*, 2014, **25**,3179-3189.

9 H.P. Yang, S. Wu, Y.P. Duan, X.F. Fu, J.M. Wu, *Appl. Surf. Sci.*, 2011, **258**, 3012-3018.

10 C.W. Liu, H.B. Chen, K. Dai, A.F. Xue, H. Chen, Q.Y. Huang, *Mater. Res. Bull.*, 2013, **48**, 1499-1505.

11 H. Wang, H.L. Wang, W.F. Jiang, Z.Q. Li, *Water Res.*, 2009, **43**, 204-210.

12 A. Jitianu, T. Cacciaguerra, R. Benoit, S. Delpeux, F. Beguin, S. Bonnamy, *Carbon*, 2004, **42**, 1147-1151.

13 Y. Yu, J.C. Yu, C.Y. Chan, Y.K. Che, J.C. Zhao, L. Ding, *Appl. Catal. B.*, 2005, **61**, 1-11.

14 T.A. Saleh, V.K. Gupta, *J. Colloid Interface Sci.*, 2011, **362**, 337-344.

15 W.D. Wang, P. Serp, P. Kalck, J.L. Faria, *J. Mol. Catal. A: Chem.*, 2005, **235**, 194-199.

16 K. Dai, X.H. Zhang, K. Fan, T.Y. Peng, B.Q. Wei, *Appl. Surf. Sci.*, 2013, **270**, 238-244.

17 K. Dai, T.Y. Peng, D.N. Ke, B.Q. Wei, *Nanotechnology*, 2009, **20**, 125603.

18 K. Woan, G. Pyrgiotakis, W. Sigmund, *Adv. Mater.*, 2009, **21**, 2233-2239.

19 Y. Yao, G. Li, S. Ciston, R.M. Lueptow, K.A. Gray, *Environ. Sci. Technol.*, 2008, **42**, 4952-4957.

20 H.R. Jafry, M.V. Liga, Q.L. Li, A.R. Barron, *New J. Chem.*, 2011, **35**, 400-406.

21 W. Zhou, K. pan, Y. Qu, F.F. Sun, C.G. Tian, Z.Y. Ren, G.H. Tian, H.G. Fu,

Chemosphere, 2010, **81**, 555-561.

22 K. Vajda, K. Mogyorosi, Z. Nemeth, K. Hernadi, L. Forro, A. Magrez, A. Dombi, *Phys. Status Solidi B*, 2011, **248**, 2496-2499.

23 G.H. Jiang, X.Y. Zheng, Y. Wang, T.W. Li, X.K. Sun, *Powder Technol.*, 2011, **207**, 465-469.

24 N. Patel, R. Jaiswal, T. Warang, G. Scarduelli, A. Dashora, B.L. Ahuja, D.C. Kothari, A. Miotello, *Appl. Catal. B.*, 2014, **150–151**, 74-81.

25 Y. Gurkan, N. Turkten, A. Hatipoglu, Z. Cinar, *Chem. Eng. J.*, 2012, **184**, 113-124.

26 H. Chen, S. Yang, K. Yu, Y.M. Yu, C. Sun, *J. Phys. Chem. A.*, 2011, **115**, 3034-3041.

27 P.H. Chen, Y.S. Huang, W.J. Su, K.Y. Lee, K.K. Toing, *Mater. Chem. Phys.*, 2014, **143**, 1378-1383.

28 S.H. Wang, L.J. Ji, B. Wu, Q.M. Gong, Y.F. Zhu, J. Liang, *Appl. Surf. Sci.*, 2008, **255**, 3263-3266.

29 L.W. Zhang, H.B. Fu, Y.F. Zhu, *Adv. Funct. Mater.*, 2008, **18**, 2180-2189.

30 H.M. Heise, R. Kuckuk, A.K. Ojha, A. Srivastava, V. Srivastava, B.P. Asthana, *J. Raman Spectrosc.*, 2009, **40**, 344-353.

31 S.H. Liu, H.R. Syu, *Appl. Energy*, 2012, **100**,148-154.

32 G.M. An, W.H. Ma, Z.Y. Sun, Z.M. Liu, B.X. Han, S.D. Miao, Z.J. Miao, K.L. Ding, *Carbon*, 2007, **45**, 1795-1801.

33 A.V. Emeline, V.N. Kuznetsov, V.K. Rybchuk, N. Serpone, *Int. J. Photoenergy*, 2008, 258394.

34 T.Y. Peng, D. Zhao, K. Dai, W. Shi, K. Hirao, *J. Phys. Chem. B*, 2005, **109**, 4947-4952.

35 J. Yang, Q.L. Dong, Z.T. Jiang, J. Zhang, *Chin. Phys. B*, 2010, **19**, 127104.

36 S. Bagwasi, Y.X. Niu, M. Nasir, B.Z. Tian, J.L. Zhang, *Appl. Surf. Sci.*, 2013, **264**, 139-147.

37 H.Y. Wang, Y.C. Yang, J.H. Wei, L. Le, Y. Liu, C.X. Pan, P.F. Fang, R. Xiong, J. Shi, *Reac. Kinet. Mech. Cat.*, 2012, **106**, 341-353.

38 A. Kongkanand, P.V. Kamat, *ACS Nano*, 2007, **1**, 13-21.

39 D. Nassoko, Y.F. Li, H. Wang, J.L. Li, Y.Z. Li, Y. Yu, *J. Alloys Compd.*, 2012, **540**, 228-235.

Captions for Tables and Figures

Table 1 Summary of the physicochemical properties of TiO_2, 5 wt% SWCNT-TiO_2, N/TiO_2 and SWCNT-N/TiO_2 hybrids.

Figure 1. X-ray diffraction patterns of TiO_2, N/TiO_2, 5 wt% SWCNT-TiO_2 and SWCNT-N/TiO_2 hybrids with different contents of SWCNTs.

Figure 2. (a) UV–vis diffuse reflection spectra of TiO_2, N/TiO_2, SWCNT-TiO_2 and the SWCNT-N/TiO_2 hybrids with different contents of SWCNTs; (b) Plot of $(\alpha h\nu)^{1/2}$ versus photon energy ($h\nu$) according to the DRS in (a).

Figure 3. SEM images of the 2.5 wt% SWCNT-TiO_2 (a) and 2.5 wt% SWCNT-N/TiO_2 (b); TEM images of the 2.5 wt% SWCNT-N/TiO_2 (c and d).

Figure 4. Raman spectrum of TiO_2, SWCNT, SWCNT-TiO_2 and SWCNT-N/TiO_2 hybrid.

Figure 5. XPS spectra for the SWCNT-N/TiO_2 hybrid: survey (a), C 1s (b), Ti 2p (c), O 1s (d), and N 1s (e).

Figure 6. Photocatalytic degradation efficiencies of sulfathiazole over different photocatalysts under visible light irradiation (a: photolysis, b: TiO_2, c: 5 wt% SWCNT-TiO_2, d: 5 wt% SWCNT+N/TiO_2, e: N/TiO_2, f: 5 wt% MWCNT-N/TiO_2, g: 5 wt% DWCNT-N/TiO_2, h: 5 wt% SWCNT-N/TiO_2).

Figure 7. Photocatalytic degradation efficiencies of sulfathiazole over SWCNT-N/TiO_2 hybrids with different contents of SWCNTs under visible light irradiation. (a: 10 wt% SWCNT-N/TiO_2, b: 1.25 wt% SWCNT-N/TiO_2, c: 2.5 wt% SWCNT-N/TiO_2, d: 5 wt% SWCNT-N/TiO_2).

Figure 8. Proposed mechanism for photocatalytic degradation of sulfathiazole over the SWCNT-N/TiO_2 hybrid; S: sulfathiazole; S_{ox}: oxidized sulfathiazole.

Table 1 Summary of the physicochemical properties of TiO_2, N/TiO_2, 5 wt% SWCNT–TiO_2, and SWCNT-N/TiO_2 hybrids.

Samples	Crystallite size (nm)	λ (nm)	E_g (eV)
TiO_2	18.1[16]	400	3.1
5 wt% SWCNT-TiO_2	11.2[16]	428	2.90
N/TiO_2	9.6	530	2.34
1.25 wt% SWCNT-N/TiO_2	14.6	449	2.76
2.5 wt% SWCNT-N/TiO_2	10.2	561	2.21
5 wt% SWCNT-N/TiO_2	11.4	432	2.87
10 wt% SWCNT-N/TiO_2	10.1	504	2.40

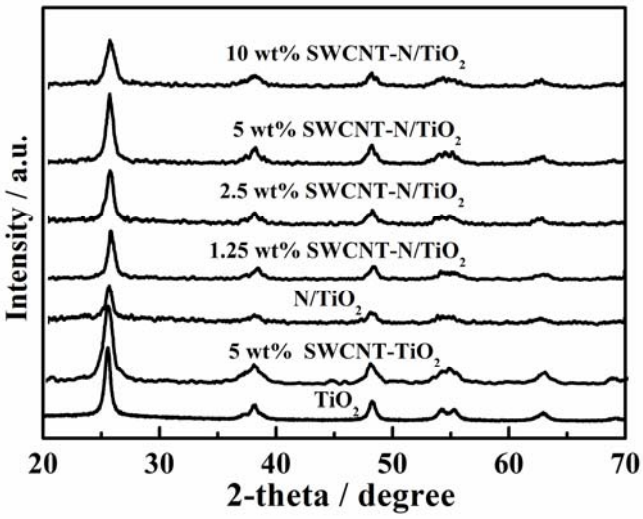

Figure 1. X-ray diffraction patterns of TiO_2, N/TiO_2, 5 wt% SWCNT-TiO_2 and SWCNT-N/TiO_2 hybrids with different contents of SWCNTs.

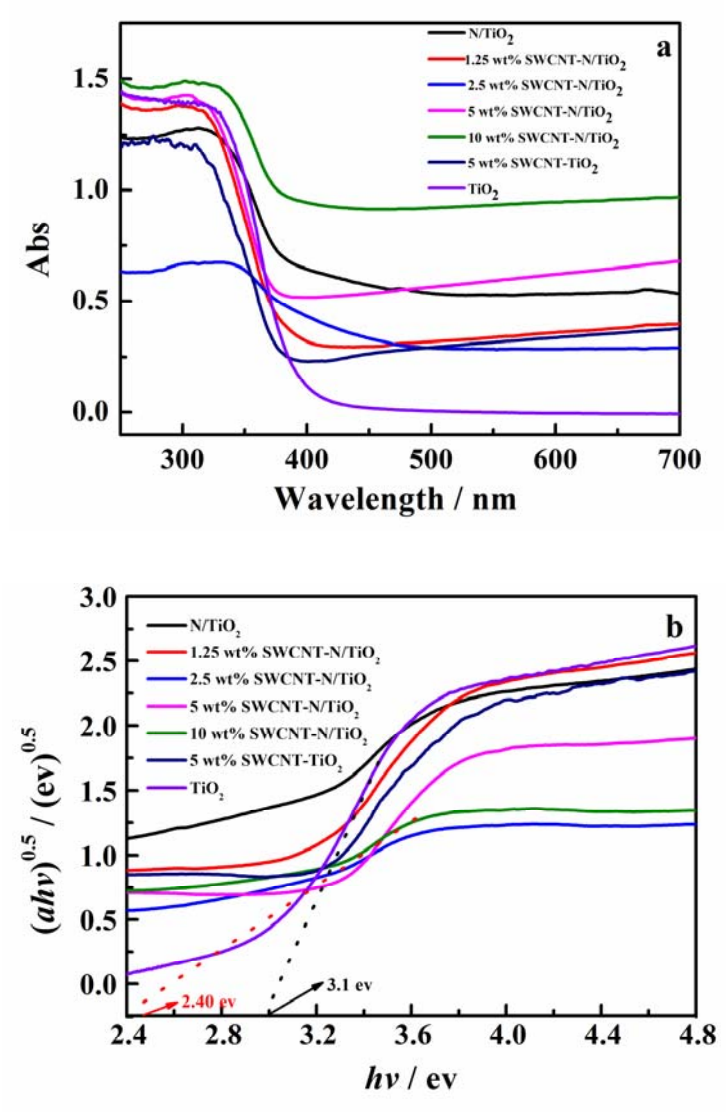

Figure 2. (a) UV–vis diffuse reflection spectra of TiO_2, N/TiO_2, SWCNT-TiO_2 and the SWCNT-N/TiO_2 hybrids with different contents of SWCNTs; (b) Plot of $(\alpha h\nu)^{1/2}$ versus photon energy ($h\nu$) according to the DRS in (a).

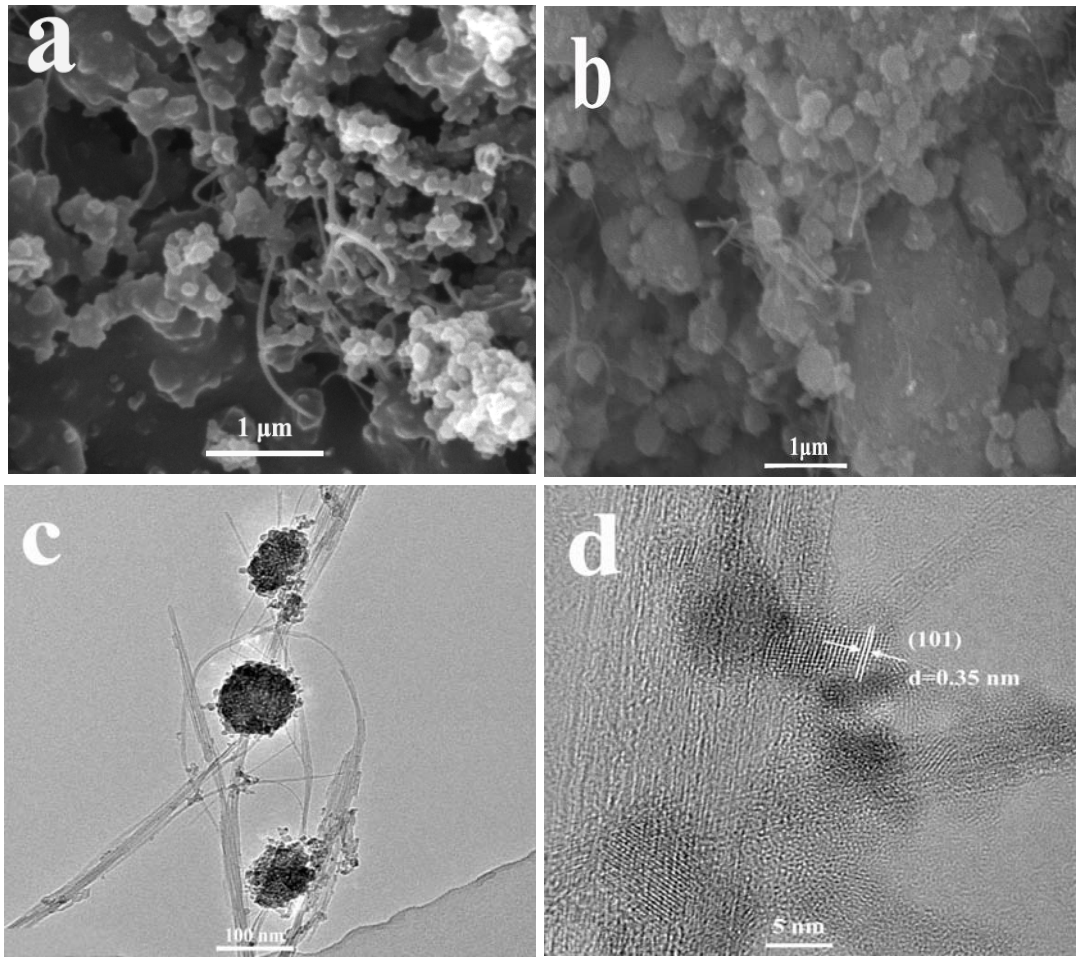

Figure 3. SEM images of the 2.5 wt% SWCNT-TiO_2 (a) and 2.5 wt% SWCNT-N/TiO_2 (b); TEM images of the 2.5 wt% SWCNT-N/TiO_2 (c and d).

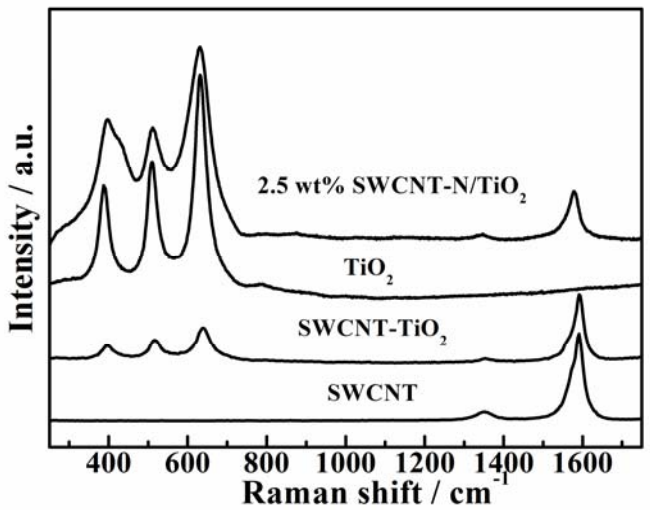

Figure 4. Raman spectrum of TiO_2, SWCNT, SWCNT-TiO_2 and SWCNT-N/TiO_2 hybrid.

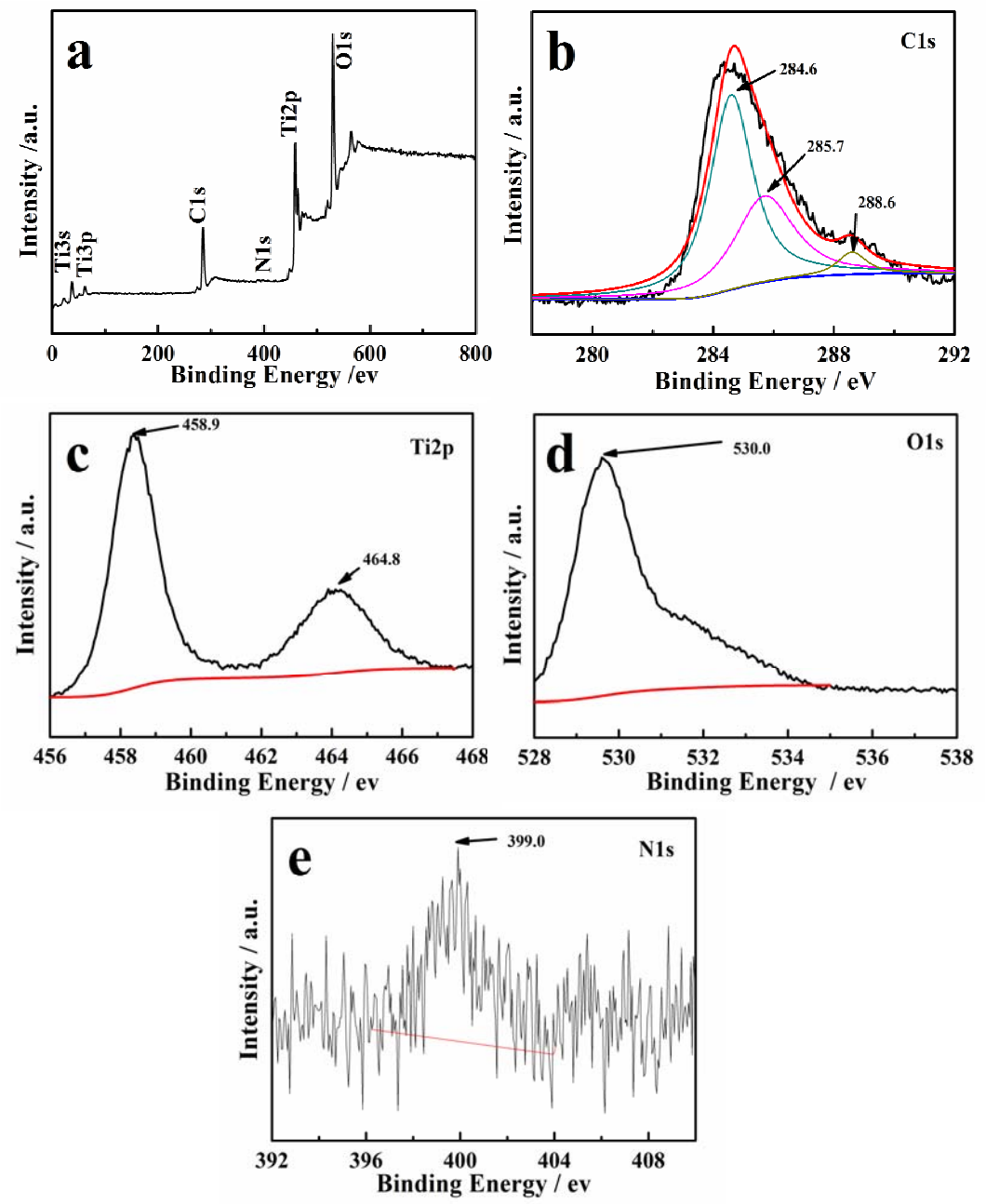

Figure 5. XPS spectra for SWCNT-N/TiO_2 hybrid: survey (a), C 1s (b), Ti 2p (c), O 1s (d), and N 1s (e).

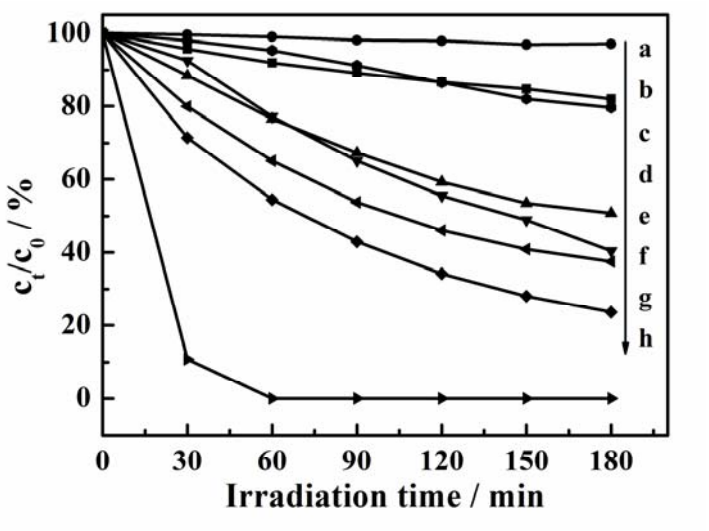

Figure 6. Photocatalytic degradation efficiencies of sulfathiazole over different photocatalysts under visible light irradiation (a: photolysis, b: TiO_2, c: 5 wt% SWCNT-TiO_2, d: 5 wt% SWCNT+ N/TiO_2, e: N/TiO_2, f: 5 wt% MWCNT-N/TiO_2, g: 5 wt% DWCNT-N/TiO_2, h: 5 wt% SWCNT-N/TiO_2).

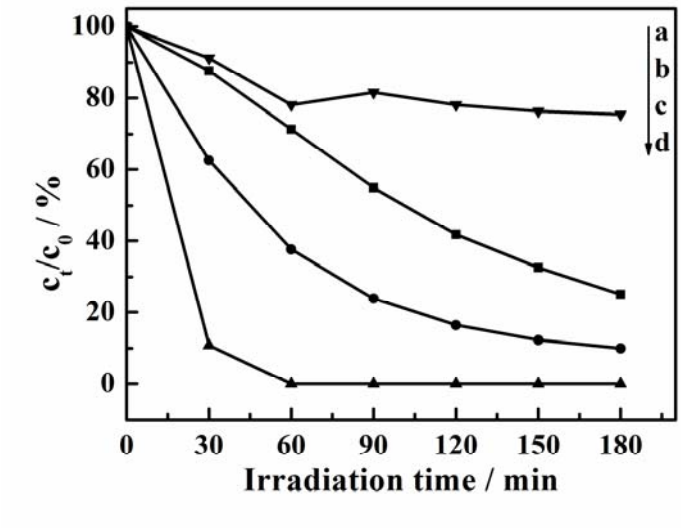

Figure 7. Photocatalytic degradation efficiencies of sulfathiazole over SWCNT-N/TiO_2 hybrids with different contents of SWCNTs under visible light irradiation. (a: 10 wt% SWCNT-N/TiO_2, b: 1.25 wt% SWCNT-N/TiO_2, c: 2.5 wt% SWCNT-N/TiO_2, d: 5 wt% SWCNT-N/TiO_2).

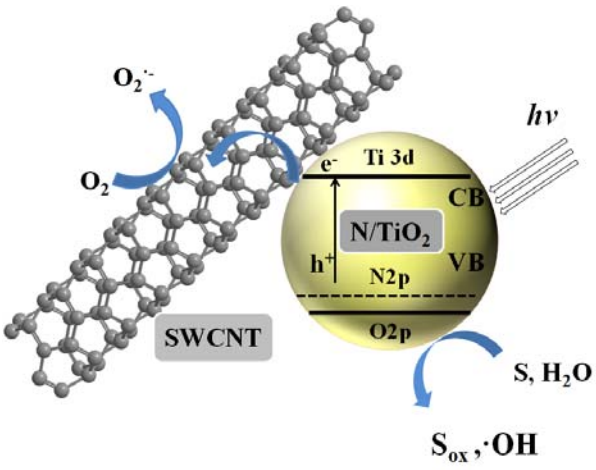

Figure 8. Proposed mechanism for photocatalytic degradation of sulfathiazole over the SWCNT-N/TiO_2 hybrid; S: sulfathiazole; S_{ox}: oxidized sulfathiazole.

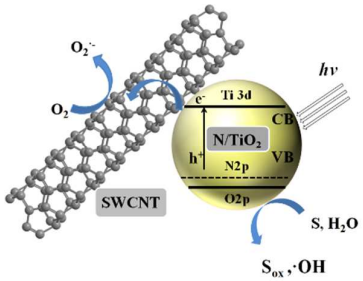

Synergetic effects of SWCNT modification and N doping generate superior visible-light-induced photocatalytic activity of SWCNT-N/TiO_2 to MWCNT-N/TiO_2 and DWCNT-N/TiO_2.